Tuijin Jishu/Journal of Propulsion Technology
ISSN: 1001-4055
Vol. 45 No. 3 (2024)

Optimizing Solar Energy Prediction: Insights from Comparative Analysis of Models, Optimizers, and Performance Evaluation

Ami T. Patel[1]*, Nikunj J. Dhimmar[1]
[1]*Department of Electrical Engineering, Government Engineering College, Bharuch, Gujarat, India*

Abstract:- This research aimed to enhance solar energy prediction accuracy through a comparison of models and optimization techniques. Long Short Term Memory and Recurrent Neural Network models were analyzed using nine features extracted from Typical Meteorological Year 3 format data obtained from National Solar Radiation Database, revealing distinctive patterns in seasonal variations and temporal availability of solar energy. Integration of Recurrent Neural Networks and Long Short Term Memory models significantly improved performance, addressing limitations in capturing long-term dependencies and uncertainties. Long Short Term Memory consistently outperformed other metrics by 2-3%, with larger hidden layer sizes enhancing predictive accuracy. The importance of selecting the appropriate optimizer considering accuracy, computational resources, and training time constraints was emphasized. Project-specific analysis underscored the significance of tailoring solar dimensions to location-specific yield data, informing cost optimization strategies for sustainable development.

Keywords:- Artificial Neural Network, Estimation, Optimizer, Performance Evaluation

1. Introduction

Global energy demand is rising due to industrial and population growth, primarily met by fossil fuels. However, increasing concerns about climate change necessitate a transition to renewable energy sources like solar power. Solar energy's unpredictability requires efficient utilization, achieved by accurately sizing solar energy systems. Machine learning facilitates precise prediction of solar energy output, optimizing its utilization (1). Computer methods like Artificial Neural Networks (ANNs) and Fuzzy Logic (FL) excel at understanding solar energy's variability, enabling accurate estimation of solar panel output (2).

This research focuses on the use of ANN methods to address issues with solar energy. Various types of ANNs exist, each with unique strengths, but one will be selected that considers different factors to estimate solar energy potential. This will help us set up solar systems in the best possible way(3). Solar energy, mainly from the sun, is an important renewable source. Installing solar panels needs careful sizing for best results, as highlighted by companies like GRIDSCAPE Solutions. Efficient solar power utilization depends on accurate sizing informed by weather data. Traditional estimation methods face challenges due to complex math, resource demands, and data quality issues. Machine learning offers a solution, providing faster and more precise estimates by deriving patterns from real data (4). This research aims to develop an ANN model for accurate solar potential estimation, especially in data-scarce regions like India, using empirical correlations from measured meteorological parameters to enhance understanding for solar energy deployment.

2. Estimation of PV Power

Various methods have been proposed to estimate the power output of photovoltaic (PV) systems(5). These methods use factors like irradiation and ambient temperature from meteorological agencies for PV power generation prediction, showing high correlation. Even with just irradiation and ambient temperature, PV power output remains consistent as shown in equation(1), converted from [MJ/m^2] data provided by meteorological agencies (6).

$$1\ \frac{MJ}{m^2} = \frac{1}{3.6}\ \frac{kWh}{m^2} \tag{1}$$

The daily PV power capacity estimate can be derived from meteorological data and represented as follows.

$$P_{PV} = \frac{S}{3.6*i} * A_{module} * N * \eta_{module}\ \frac{kWh}{day} \tag{2}$$

From equation (2), S represents the daily irradiation data provided in [MJ/m^2], A_{module} stands for the area of the PV module, N denotes the number of PV modules, η_{module} represents the energy conversion efficiency of the PV module, and i is the climate variation factor influencing PV power generation due to environmental conditions like clouds, fog, etc(7). PV power output drops with higher temperatures due to semiconductor properties is expressed as follows.

$$P_{PV(t)} = PV_{max,ref}\ \frac{G_T}{G_{ref}}\left(1 - \beta(t_m - 25)\right) \tag{3}$$

In equation (3) $PV_{max,ref}$ represents the peak power output of a photovoltaic (PV) system under Standard Test Conditions (STC), which include an air mass of 1.5G, 1000 W/m^2 irradiance, and a temperature of 25^0C. G_{ref} denotes the reference irradiance of 1000 W/m^2, GT denotes irradiation on the PV array plane, t_m indicates the solar module's surface temperature during operation, and the temperature coefficient of peak power signifies the percentage change per degree Celsius(8) (9).

2.1 Utilizing Artificial Neural Networks for Solar Energy Estimation

Figure 1 depicts the architecture of an Artificial Neural Network (ANN), which is utilized in solar estimation methods to predict photovoltaic (PV) generation(10)(11). These methods use neural networks to learn complex relationships between input variables (such as solar irradiance, temperature, and time of day) and PV output (12). ANN models provide accurate solar energy forecasts, aiding energy planning and system optimization (13).

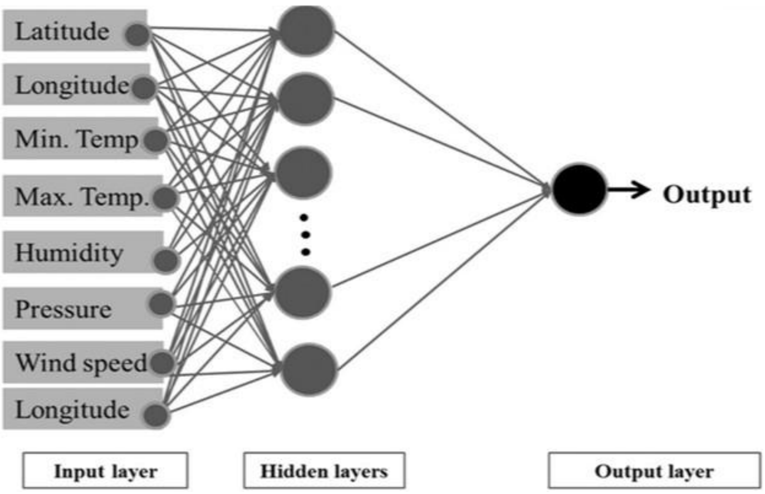

Figure 1 Structure of Artificial Neural Network

2.2 Advancing Solar Energy Estimation with Recurrent Neural Networks (RNNs)

Recurrent Neural Networks (RNNs) are a type of artificial neural network particularly suited for sequential data, making them suitable for time-series forecasting tasks like solar estimation(14). Several methods are available as a part of RNNS. Figure 2 depicts the flowchart outlining the proposed methodology for solar estimation.

2.2.1 Sequence Learning: RNNs capture sequential data patterns by retaining past inputs, making them effective for predicting future solar energy generation based on historical irradiance and other relevant data(13).

2.2.2 Temporal Dynamics: RNNs excel at capturing temporal dynamics in solar energy generation, enabling accurate predictions from sequential input data.

2.2.3 Long Short-Term Memory (LSTM): LSTM, a variant of RNNs, addresses vanishing gradients, making it effective for tasks like solar estimation, where long-term dependencies matter.

2.2.4 Model Training: RNNs, like LSTMs, are trained on historical time-series data, learning to map inputs to predictions while minimizing errors(15).

2.2.5 Prediction: Trained RNN models predict solar energy generation, assisting in energy planning and grid management, with LSTMs excelling at capturing temporal dynamics for precise estimation (13).

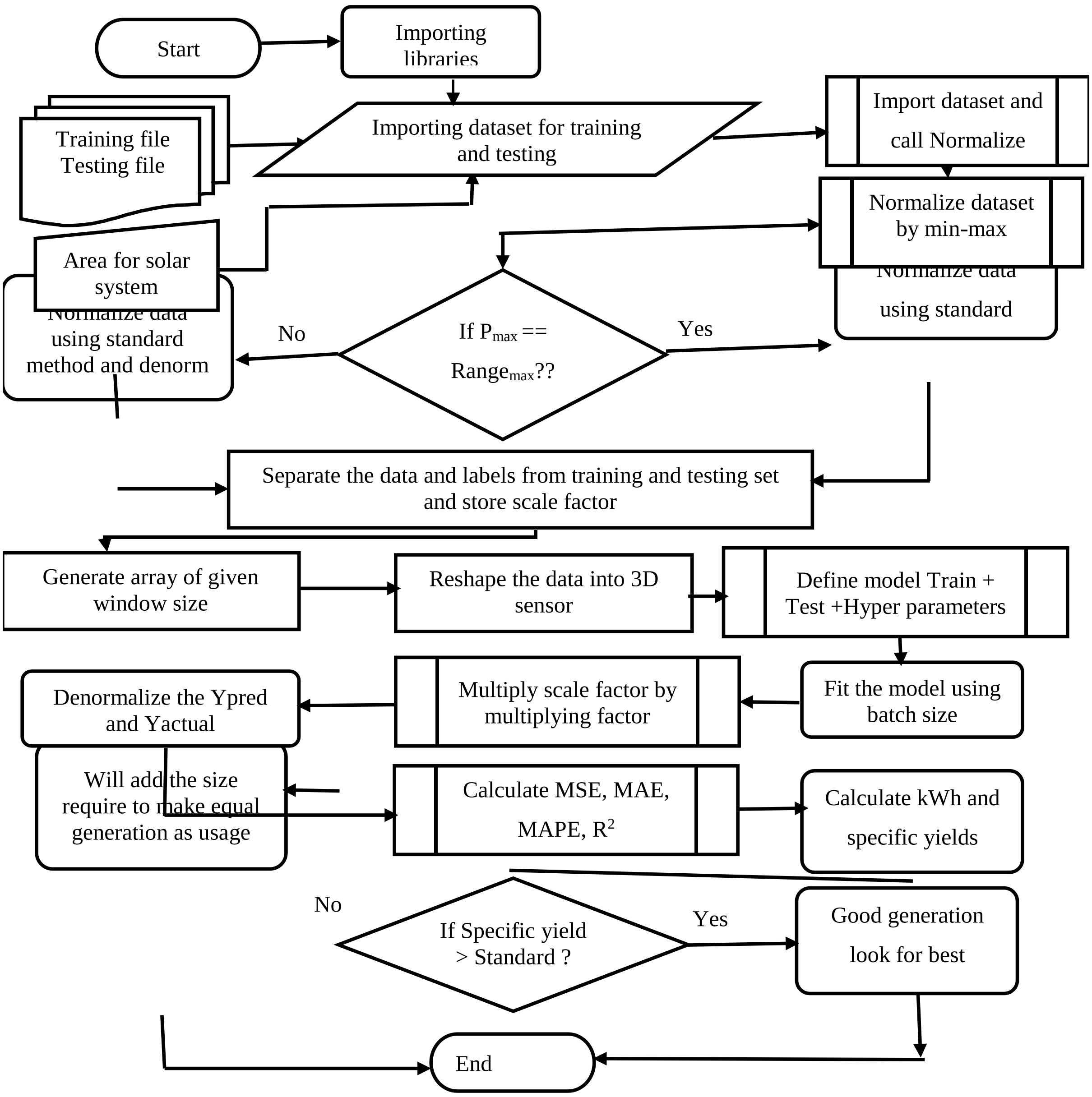

Figure 2 Flow chart of proposed methodology for solar estimation

2.3. Performance Evaluation of solar power generation

When designing a model, assessing its performance using specific measures determines prediction accuracy with the dataset; below are the measures used in this solution.

Tuijin Jishu/Journal of Propulsion Technology
ISSN: 1001-4055
Vol. 45 No. 3 (2024)

2.3.1 Mean Absolute Percentage Error (MAPE)

MAPE assesses prediction accuracy in various statistical contexts, highlighting distinct model characteristics through different percentage ranges(16). MAPE values below 10% indicate high accuracy, 10%-20% suggest good performance, 20%-50% signify reasonable capabilities, and values exceeding 50% indicate inaccurate forecasts, requiring model improvement(17). Additionally, when actual values are zero, the predicted value is considered as 1. In this case, the error ranges from 0 to 1, with 1 indicating a completely inaccurate prediction.

$$MAPE = \frac{1}{N}\sum_{i=1}^{N}\left|\frac{y_i-\widehat{y_i}}{y_i}\right| \tag{4}$$

Where y_i represents actual output and $\widehat{y_i}$ denotes estimated output. In certain models, accuracy is determined by dividing the error term by the estimated value instead of the actual value as indicated in Equation 2.

$$Accuracy = \frac{1}{N}\sum_{i=1}^{N}\left|\frac{y_i-\widehat{y_i}}{y_i}\right| \tag{5}$$

2.3.2 Mean square error (MSE)

MSE is a basic regression evaluation metric, calculating the average squared error. It's limited because it can't produce negative results. A perfect model would have an MSE of zero (18).

$$MSE = \frac{1}{N}\sum_{i=1}^{N}(y_i - \widehat{y_i})^2 \tag{6}$$

Where y_i represents actual output and $\widehat{y_i}$ denotes estimated output.

2.3.3 Mean Absolute Error (MAE)

MAE, or Mean Absolute Error, calculates the average absolute difference between values, assigning equal weight to all individual differences(11).

$$MAE = \frac{1}{N}\sum_{i=1}^{N}|y_i - \widehat{y_i}| \tag{7}$$

Where y_i represents actual output and $\widehat{y_i}$ denotes estimated output.

2.3.4 Coefficient of determination

The R^2, or coefficient of determination, stands as a pivotal technique for assessing the improvement of our model over the constant baseline(18). It quantifies our model's effectiveness compared to the naive mean model and evaluates performance regardless of scale (2). Ideally, the R^2 value should range from 0 to 1, with lower values indicating superior performance.

$$R^2 = 1 - \frac{MSE(Model)}{MSE\ (Baseline)} \tag{8}$$

$$MSE(Model) = \frac{1}{N}\sum_{i=1}^{N}(y_i - \widehat{y_i})^2 \tag{9}$$

$$MSE(Baseline) = \frac{1}{N}\sum_{i=1}^{N}(y_i - \bar{y})^2 \tag{10}$$

Where y_i represents actual output and $\widehat{y_i}$ denotes estimated output. Also $\bar{y}$ indicates Mean of the actual output, MSE (Model) stands for MSE error of the model and MSE (Baseline) represents Native error of the model.

2.4 Enhancing Neural Network Training: Exploring Optimizers for Improved Performance

Backpropagation is crucial in neural network learning. It involves calculating errors and propagating them back to improve overall model performance. However, its effectiveness can suffer when different layers learn at different rates. Optimization algorithms address this by expediting learning and minimizing error functions, thus enhancing neural network training efficiency(19). Various optimization algorithms, like Momentum, Nesterov, Adagrad, Adadelta, RMSprop, and Adam, dynamically adjust learning rates, enhancing neural network performance and training speed.

2.4.1 Gradient Descent optimization algorithm

Momentum optimizer improves Gradient Descent by addressing its slow convergence and oscillations, boosting neural network training efficiency(20). Momentum enhances Gradient Descent by introducing inertia, achieving faster convergence and improved training efficiency for neural networks by considering past updates.

2.4.2 Root Mean Square Propagation Optimizer

RMSprop adjusts learning rates adaptively based on the square root of the exponentially decaying average of squared gradients, addressing issues like vanishing or exploding gradients in neural network training, resulting in stable and efficient training for improved performance (21).

2.4.3 Adaptive Gradient Algorithm optimizer

Adagrad, or Adaptive Gradient Algorithm, optimizes neural network training by adaptively adjusting the learning rates of individual parameters based on their historical gradients (22). This optimizer adjusts learning rates based on past gradients, favoring frequent parameter updates but risks continuous rate decrease and premature convergence. So, it's often complemented with other algorithms or learning rate decay strategies (17).

2.4.4. Adadelta optimization algorithm

Adadelta dynamically adjusts learning rates based on past gradients and updates, overcoming Adagrad's issue of decreasing rates, ensuring stable and efficient training, especially in sparse data or noisy gradients (23).

2.4.5 Adaptive Moment Estimation

Adam merges momentum and RMSprop for efficient optimization, dynamically adjusting learning rates based on past gradients and squared gradients, enhancing neural network training [24]. Its adaptive learning rate accelerates convergence and ensures stability by analyzing parameter changes, outperforming older methods with fewer adjustments.

3. Results and discussion

LSTM and RNN models are employed for solar generation estimation, optimizing configurations and features across 9 parameters. Data retrieval follows the TMY3 format, sourced from the NSRDB via PV_{Watts}, providing seasonal patterns from 2006 to 2020. This data, post-processing, is transformed into CSV files for diverse applications.

3.1 Comparative Assessment of Regression Analyses for Solar Energy Prediction

To understand the nonlinear behaviour of the data influenced by various factors, Feed Forward Neural Network (FFNN) regression analysis was initially applied. This analysis examined correlations in annual data from the same state, country, or globally, revealing seasonal patterns and solar energy availability. Models trained on diverse datasets showed improved accuracy. Additionally, normalization or standardization techniques were explored, especially in relation to tropical data. Weather profiles investigated include Baroda and Hyderabad in Gujarat, India; Gangtok, India; and Fremont, California, USA. Table 1 presents solar energy generation data for four weather profiles (Weather Profile 1, 2, 3, and 4), along with combined data from all weather files.

Table 1 Comparative Assessment of Regression Analyses

	Different city in different state in different country				
	Different city in different state in same country				
	Different city in same state				
CSV data city	**Weather Profile 1**	**Weather Profile 2**	**Weather Profile 3**	**Weather Profile 4**	**Combined all weather file**
Expected	**Derived outcome**				

outcome					
609.733	597.47	582.94	611.34	652.19	606.06689
%	2.01	4.39	-0.26	-6.96	0.6
38647.11	38511.4	38207.17	38722	39030.07	38730.516
%	0.35	1.14	-0.19	-0.99	-0.22
8889.068	8863.89	8844.63	8910.12	8910.52	8891.1523
%	0.28	0.5	-0.24	-0.24	-0.02
28697.84	28755.83	28640.74	28739.68	28742.99	28677.725

It includes "Expected outcome" values representing anticipated solar energy generation and "Derived outcome" values showing actual observed values. The percentage difference between expected and derived outcomes indicates prediction accuracy. This table offers insights into geographical variations and factors influencing solar energy production in different regions.

3.2 Integrating RNN and LSTM Models

The RNN model, trained via mini-batch gradient descent, struggles with uncertainty, causing inaccuracies, especially in steep declines in solar generation. LSTM resolves this with long-term dependency retention. The Simple RNN structure uses window sizes of (1, 5, 24, 48) with a batch size of 16, while the RNN-LSTM structure incorporates LSTM layers to improve capturing long-term dependencies in the data, employing window sizes of (1, 5, 10, 24, 48) with batch sizes of (16, 32, 64). Both structures are trained using the Adam optimizer with varying window sizes and batch sizes to explore different temporal perspectives and optimize model performance.

3.3 Performance Evaluation of parameters

When evaluating model performance, error-based methods are crucial, with MAPE being widely preferred. While MSE, MAE, and R^2 are straightforward to implement, incorporating MAPE requires assumptions about non-solar and solar hours. To effectively apply MAPE, a loop structure is devised. When encountering non-solar hours where the model predicts solar generation, LSTM prediction is treated as 1; otherwise, it's considered 0.

Table 2 Analysis of performance evaluation parameters

Window	**MSE (Watts)**	**MAE (Watts)**	**R^2 (%)**	**MAPE (0 to 1)**	**Note**	**Train data size**
1	706406.6	4595125	93.35	0.3216	Month, Day, Hour	(87600,1,3)
1	932148.9	5159518	91.23	0.4903	Wind Speed (m/s)	(87600,1,4)
1	960190	5749101	90.96	0.4621	Wind Speed (Beaufort)	(87600,1,4)
1	1444707.8	7895388	86.42	0.6486	Added a temp with WS(m/s)	(87600,1,5)
1	1003147.5	6836478	90.56	1.1106	Added cell temperature	(87600,1,6)

1	583331.3	5149877	94.51	0.8877	Added direct irradiance	(87600,1,7)
1	861108.1	6802453	91.9	0.3062	Added diffuse irradiance	(87600,1,8)
1	315256.2	3394112	97.03	0.2742	Added POA irradiance	(87600,1,9)
5	513861.8	4577444	95.16	0.9858	Whole model data	(87600,1,9)
10	344638.7	3731452	96.76	0.5462	Whole model data LSTM	(87600,1,9)
24	350119.1	3708279	96.7	0.1212	Whole model data LSTM	(87600,1,9)
24	350119.1	3708279	96.7	0.1212	Whole model data LSTM	(87600,1,9)
48	258243.8	2898061	97.57	0.2596	Whole model data LSTM	(87600,1,9)
1	350374.1	3651782	96.7	0.2736	Replaced LSTM with Simple RNN	(87600,1,9)
24	387688.1	4105181	96.35	0.1495	Replaced LSTM with Simple RNN	(87600,1,9)

Table 2 displays experiments with diverse window sizes and model set ups, comparing features like wind speed, temperature, and irradiance, as well as different architectures like LSTM and Simple RNN. These comparisons offer insights into model performance across various conditions, aiding in the identification of optimal configurations for precise solar energy generation prediction.

3.4 Comparative Analysis of Optimizer Selection

Table 3 shows that SGD, a popular optimization method for training neural networks, resulted in bigger errors compared to other methods, as seen in its relatively high MSE and MAE values. However, it's R^2 score of 84.2% suggests it still has a decent ability to make predictions. The MAPE value is relatively high at 0.65544, indicating a notable percentage error in predictions. Training time is reasonable at 58.391 seconds.

Table 3 Optimizer selection

Optimiser	MSE	MAE	R^2	MAPE	time
SGD	2833787	14075091	84.2	0.65544	58.391
RMSprop	1236112	7191423	93.11	0.34894	59.983
adagrade	1226473	6996371	93.16	0.24687	60.303
adadelta	954853	5007534	94.67	0.23359	60.351
adam	117677	6477337	93.77	0.32556	63.89

RMSprop, suitable for non-stationary problems, reduces MSE and MAE compared to SGD, yielding a higher R^2 score of 93.11% and a lower MAPE value of 0.34894 in 59.983 seconds. Adagrad achieves similar results with a slightly higher R^2 score of 93.16%, lower MAPE value of 0.24687, and comparable training time of 60.303 seconds. Adadelta resolves diminishing learning rates, achieving lower MSE and MAE, with a higher R^2 score of 94.67%, lower MAPE value of 0.23359, and slightly higher training time of 60.351 seconds. Adam combines Adagrad and RMSprop benefits, yielding the lowest MSE and MAE, highest R^2 score of 93.77%, and relatively low MAPE value of 0.32556, but requires the longest training time at 63.89 seconds. The choice depends on accuracy, computational resources, and time constraints, where Adam excels in accuracy but takes longer to train, while RMSprop and Adadelta offer competitive results with lower training times.

Hidden layers are represented as h1, h2, h3 respectively. From Table 4 depicts that the models with higher values of h2 and h3 generally exhibit improved predictive accuracy and lower error metrics, suggesting that increasing the complexity of the model by adding more hidden layers and units can enhance its ability to capture complex patterns in the data.

Table 4 Model Architecture Evaluation

h1	h2	h3	MSE	MAE	R^2	MAPE	time
1	1	1	3974327	18383718	77.85	0.8097	55.324
9	1	1	1653214	9034113	90.78	0.4659	59.271
9	9	1	1278925	7084613	92.87	0.3253	55.47
9	9	9	1171145	6603040	93.47	0.3367	57.205
9	16	16	1174168	6676310	93.45	0.3099	62.777
9	32	32	1293386	7453939	92.79	0.34	59.501
9	64	64	1117678	6477337	93.77	0.3255	63.89
9	64	64	1158578	6648973	93.54	0.4361	60.594

The model with h1=9, h2=64, and h3=64 consistently outperforms other configurations across various metrics. It achieves the lowest MSE (1,117,678), MAE (6,477,337), and MAPE (0.3255), as well as the highest R^2 (93.77%) among all configurations. Training time increases with model complexity, especially with higher values of h2 and h3, although differences between configurations are minor. The configuration with h1=9, h2=64, and h3=64 balances predictive accuracy and computational efficiency, emerging as the optimal choice. However, hyperparameters should be chosen carefully based on specific application requirements and constraints.

3.5 Analysis Based on Project Selection

The selection of solar project size and parameters relies on specific yield, determined by kWh simulated by the model in Table 5, reflecting actual performance at a location. With three models oriented south, southeast, and southwest, each with a 15 kW size, tailored for specific azimuth directions, their annual generation is evaluated at approximately 1700, 1400, and 1600 specific yield values. The 15 kW systems aim to generate 24019 kWh annually at a standard yield of 1600. NPV and IIR over a 30-year period are scrutinized to compare cash flow in present-day terms and gauge return from NPV cash flows, respectively, considering inflation, interest, and costs.

Table 5 Refining Solar Sizing: Tailoring Dimensions through Specific Yield Analysis

kWh generated			Specific yield			KW size needed		
case 1	case 2	case 3	case 1	case 2	case 3	case 1	case 2	case 3
26006	21556	25361	1734	1437	1691	13.85	16.71	14.2
25230	21771	25260	1682	1451	1684	14.28	16.54	14.26
26213	20976	24958	1748	1398	1664	13.74	17.17	14.43

Table 6 underscores the significance of customizing solar dimensions to location-specific yield data (specific yield of 1600), improving project cost-effectiveness and facilitating the selection of projects with higher NPV. Objectives include minimizing costs, prioritizing high-yield locations, and optimizing space usage. While an ESS may not be necessary, its installation can be considered for efficient generation management and optimal performance.

Table 6 Project Cost Optimization: Strategies and Analysis

	c_1 Default	c_1 Reduced	c_2 Default	c_2 Reduced	c_3 Default	c_3 Reduced
Payments	$1,99,166	$1,89,810	$1,99,166	$2,13,202	$1,99,166	$1,91,681
Bill saving	$4,60,761	$4,47,305	$4,01,951	$4,41,865	$4,56,170	$4,47,910
IIR	5.77%	5.93%	4.69%	4.90%	5.69%	5.86%
NPV	$20,211	$23,162	($7,789)	($2,821)	$18,025	$21,578
Payback	15.3	15	17.1	16.7	15.4	15.1
Savings/M	11178	10852	9752	10719	11065	10865

4. Conclusion

This research offers valuable insights into improving solar energy prediction accuracy through thorough evaluation. Integrating LSTM models consistently outperforms traditional methods, enhancing accuracy by 2-3%. Exploring diverse architectures and optimizers reveals configurations balancing accuracy and efficiency, with the Adam optimizer excelling. Tailoring project selection to location-specific data and cost optimization strategies maximizes project viability and sustainability, driving the transition to renewable energy.

This research highlights the vital role of rigorous performance evaluation in advancing solar energy prediction. Through continuous refinement of modeling techniques and optimization strategies based on empirical data, renewable energy adoption can be accelerated. Achieving an accuracy level of approximately 95-96% for the Indian profile underscores the significance of ongoing research efforts in supporting the transition to a more sustainable energy future.

Nomenclature

ADAM	Adaptive Moment estimation	**LR**	Learning Rate
ANFIS	Adaptive Neuro - Fuzzy Inference System	**LSTM**	Long Short Term Memory
ANN	Artificial Neural Network	**MAE**	Mean Absolute Error
AOI	Angle Of Incident	**MAPE**	Mean Absolute Percentage Error
ASHRAE	American Soc. of Heating, Refrigeration & Air-conditioning Engineers	**MSE**	Mean Square Error
BP	Back Propagation	**NN**	Neural Network
CNN	Convolutional Neural Network	**NREL**	National Renewable Energy Laboratory
DHI	Direct Horizontal Irradiance	**POA**	Plane Of Array
DNI	Direct Normal Irradiance	**R2**	Coefficient of determination
DSR	Daily Solar Irradiance	**RELU**	Rectifier Linear Unit

ESS	Energy Storage System	**RNN**	Recurrent Neural Network
FFNN	Feed – Forward Neural Network	**SAM**	System Adviser Model
FL	Fuzzy Logic	**SC**	Soft Computing technique
GA	Genetic Algorithm	**SGD**	Stochastic Gradient Descent
GHI	Global Horizontal Irradiance	**SSC**	SAM Simulation Core
ISHRAE	Indian Soc. of Heating, Refrigeration & Air-conditioning Engineers	**TANH**	Tangent Hyperbolic
IWEC	Indian Weather for Energy Calculation	**TMY**	Typical Meteorological Year

Acknowledgement

This research work is financially supported by the Director of Technical Education, Government of Gujarat under the STEM research promotion grant No./DTE/Research Promotion/STEM/LA/2021-22/11772 dated 10/12/2021. Date of commencement of project: 01/04/2022

Conflict of Interest

The authors declare that they have no known competing financial interests or personal relationships that could have appeared to influence the work reported in this paper.

References

[1] 1. Lee D, Kim K. Recurrent neural network-based hourly prediction of photovoltaic power output using meteorological information. Energies. 2019;12(2).

[2] 2. Pang Z, Niu F, O'Neill Z. Solar radiation prediction using recurrent neural network and artificial neural network: A case study with comparisons. Renew Energy. 2020;156:279–89. Available from: https://doi.org/10.1016/j.renene.2020.04.042

[3] 3. Yadav AK, Chandel SS. Solar radiation prediction using Artificial Neural Network techniques: A review. Renew Sustain Energy Rev. 2014;33:772–81.

[4] 4. Pedro HTC, Coimbra CFM. Assessment of forecasting techniques for solar power production with no exogenous inputs. Sol Energy. 2012;86(7):2017–28. Available from: http://dx.doi.org/10.1016/j.solener.2012.04.004

[5] 5. Lee HG, Kim GG, Bhang BG, Kim DK, Park N, Ahn HK. Design Algorithm for Optimum Capacity of ESS Connected with PVs under the RPS Program. IEEE Access. 2018;6:45899–906.

[6] 6. Pan X, Zhou J, Sun X, Cao Y, Cheng X, Farahmand H. A hybrid method for day-ahead photovoltaic power forecasting based on generative adversarial network combined with convolutional autoencoder. IET Renew Power Gener. 2023;17(3):644–58.

[7] 7. Huang CMT, Huang YC, Huang KY. A hybrid method for one-day ahead hourly forecasting of PV power output. Proc 2014 9th IEEE Conf Ind Electron Appl ICIEA 2014. 2014;5(3):526–31.

[8] 8. Gupta P, Singh R. PV power forecasting based on data-driven models: a review. Int J Sustain Eng. 2021;14(6):1733–55. Available from: https://doi.org/10.1080/19397038.2021.1986590

[9] 9. Heo Y, Kim J, Choi SG. Two-Stage Model-Based Predicting PV Generation with the

Conjugation of IoT Sensor Data. Sensors. 2023;23(22):1–15.

[10] 10.Akhter MN, Mekhilef S, Mokhlis H, Shah NM. Review on forecasting of photovoltaic power generation based on machine learning and metaheuristic techniques. IET Renew Power Gener. 2019;13(7):1009–23.

[11] 11.Das UK, Tey KS, Seyedmahmoudian M, Mekhilef S, Idris MYI, Van Deventer W, et al. Forecasting of photovoltaic power generation and model optimization: A review. Renew Sustain Energy Rev. 2018;81(August 2017):912–28. Available from: http://dx.doi.org/10.1016/j.rser.2017.08.017

[12] 12.Jailani NLM, Dhanasegaran JK, Alkawsi G, Alkahtani AA, Phing CC, Baashar Y, et al. Investigating the Power of LSTM-Based Models in Solar Energy Forecasting. Processes. 2023;11(5).

[13] 13.Lee D, Kim K. PV power prediction in a peak zone using recurrent neural networks in the absence of future meteorological information. Renew Energy. 2021;173(xxxx):1098–110. Available from: https://doi.org/10.1016/j.renene.2020.12.021

[14] 14.Abubakar M, Che Y, Faheem M, Bhutta MS, Mudasar AQ. Intelligent Modeling and Optimization of Solar Plant Production Integration in the Smart Grid Using Machine Learning Models. Adv Energy Sustain Res. 2024;2300160:1–19.

[15] 15.Venkateswaran D, Cho Y. Efficient solar power generation forecasting for greenhouses: A hybrid deep learning approach. Alexandria Eng J. 2024;91(February):222–36. Available from: https://doi.org/10.1016/j.aej.2024.02.004

[16] 16.Lai CS, Zhong C, Pan K, Ng WWY, Lai LL. A deep learning based hybrid method for hourly solar radiation forecasting. Expert Syst Appl. 2021;177(March):114941. Available from: https://doi.org/10.1016/j.eswa.2021.114941

[17] 17.Venkateswari R, Rajasekar N. Review on parameter estimation techniques of solar photovoltaic systems. Int Trans Electr Energy Syst. 2021;31(11):1–72.

[18] 18.Inman RH, Pedro HTC, Coimbra CFM. Solar forecasting methods for renewable energy integration. Prog Energy Combust Sci. 2013;39(6):535–76. Available from: http://dx.doi.org/10.1016/j.pecs.2013.06.002

[19] 19.Abdolrasol MGM, Suhail Hussain SM, Ustun TS, Sarker MR, Hannan MA, Mohamed R, et al. Artificial neural networks based optimization techniques: A review. Electron. 2021;10(21).

[20] 20.Premkumar M, Jangir P, Ramakrishnan C, Kumar C, Sowmya R, Deb S, et al. An enhanced Gradient-based Optimizer for parameter estimation of various solar photovoltaic models. Energy Reports. 2022;8:15249–85. Available from: https://doi.org/10.1016/j.egyr.2022.11.092

[21] 21.Gumar AK, Demir F. Solar Photovoltaic Power Estimation Using Meta-Optimized Neural Networks. Energies. 2022;15(22).

[22] 22.Wang J, Yang B, Li D, Zeng C, Chen Y, Guo Z, et al. Photovoltaic cell parameter estimation based on improved equilibrium optimizer algorithm. Energy Convers Manag. 2021;236:114051. Available from: https://doi.org/10.1016/j.enconman.2021.114051

[23] 23.Abdulkadirov R, Lyakhov P, Nagornov N. Survey of Optimization Algorithms in Modern Neural Networks. Mathematics. 2023;11(11):1–37.